THE MEASUREMENT OF MEAN FLOW ANGLES BETWEEN AN AUTOMOTIVE FAN AND STATOR

Gregory A. Kopp/Boundary Layer Wind Tunnel Laboratory, Faculty of Engineering, The University of Western Ontario

Robert J. Martinuzzi/Advanced Fluid Mechanics Research Group, Faculty of Engineering, The University of Western Ontario

ABSTRACT

Measurements of the mean velocity vector were conducted to determine the exit angle from an automotive engine cooling fan module. The measurements were made at 15 locations along a radius between the hub and the band. The radius investigated was located in a plane roughly half-way between the blade trailing edge and stator leading edge. A two-component laser Doppler velocimeter and a four-wire hot-wire probe were used to measure the flow fields. It was found that the results obtained from hot-wire anemometry will have significant bias errors when used to measure the velocity vectors between the fan and the stator unless phase-averaged data are obtained with the probe re-oriented by phase. The differences between the techniques occur because the distribution of instantaneous swirl angles is bi-modal. Further, the mean flow angle is close to a local minimum in the probability density function of the swirl angle. This will act to increase errors in measurement devices whose accuracy depends on flow direction (the quantity being measured) such as five-hole probes which are used in industry.

INTRODUCTION

Knowing the exit velocity directions from automotive fans are key to designing the downstream stators. Since the flow field is elliptic, the stators will influence the flow coming through the fan. In industry, the velocity fields pertaining to the radiator-fan-stator assemblies are typically measured with five-hole probes due to their ease of use and robustness. However, due to the high turbulence levels and large velocity gradients, the reliability of these five-hole measurements is uncertain.

Measurements to determine the mean swirl velocity projection and mean swirl angle from the fan blades upstream of the stator stage were conducted. Estimates of the average swirl angle, defined as that subtended by the swirl velocity projection relative to the fan axis, were obtained based on full three component resolution of the mean velocity vector. To this end, Laser Doppler Velocimetry (LDV) and Hot-Wire Anemometry (HWA) were used to measure the mean exit velocity. The objective of this work is to determine the reliability of the hot-wires in this flow field.

EXPERIMENTAL AND MEASUREMENT DETAILS

Fan Tests

Four radiator-fan-stator assemblies, designed by Siemens Automotive Inc. were tested; only the results from one of the assemblies are presented here. The assembly contains a dual fan module with the driver's side fan rotating at 2030 rpm and the passenger's side at 2400 rpm. The flow rate and fan speeds were set at the nominal design point, with the flow rate being 0.51 m^3/s. The hub diameter was 69 mm while the inner band diameter was 160 mm. The measurements were made at the Boundary Layer Wind Tunnel Laboratory. The wind tunnel is a multi-purpose facility, which can run in either an open or closed loop. It also has an adjustable roof. The tunnel roof on the inlet side was adjusted and calibrated to act as a Venturi section to permit volumetric flow measurements. The pressure loss across the radiator fan assembly was matched to the specified operating conditions. The downstream section was fitted to a diffuser onto which the fan module was attached.

The co-ordinate system and the measurement locations are shown schematically in Figure 1. The U velocity component corresponds to the axial (x) direction, the V velocity component corresponds to the radial component (vertical y- and radial directions coincide) and W corresponds to the tangential velocity component (z and tangential directions coincide). The measurements were conducted in a plane at midpoint between the blade trailing edge and the stator leading edge at 15 radial locations between the hub and the band. An additional test was also conducted along a radius at $\gamma = 24^\circ$ from the horizontal, as shown in Figure 1.
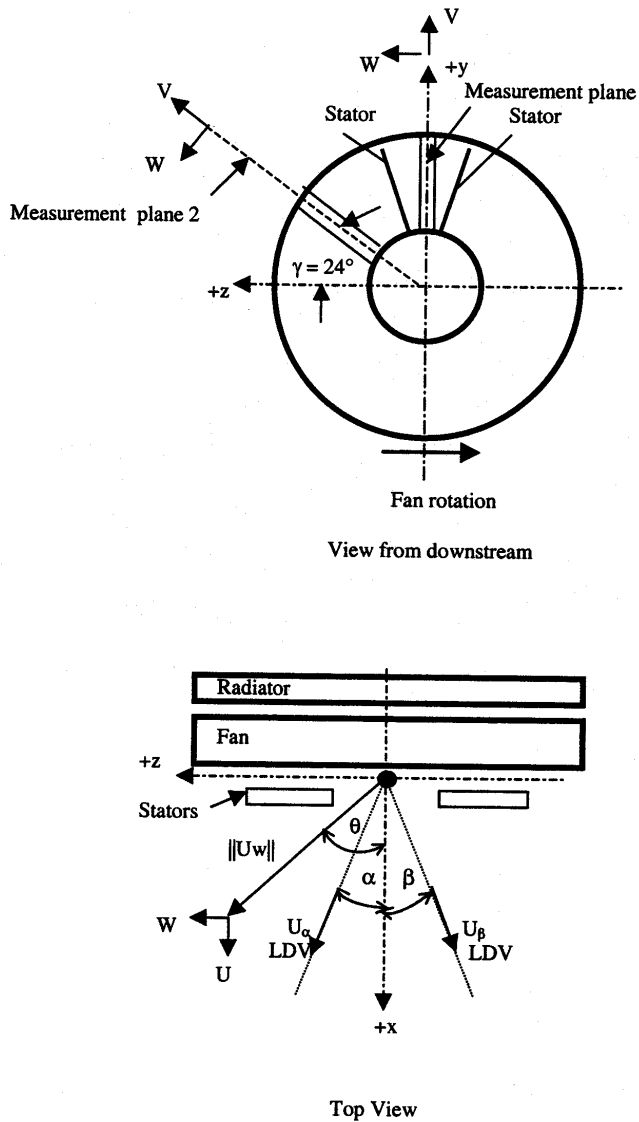
1

Copyright © 2002 by ASME

Figure 1. Schematic representation of the coordinate system and geometry.

Laser doppler velocimetry

Measurement system. Measurements were conducted with a two-component LDV. The system is a TSI Inc. model 9800 two-component fibre-optic LDV. The transmitting optics consist of a 733mm focal length, 130mm diameter lens with a 2.2x beam expander. The resulting measuring volume diameter and length, which represent the spatial resolution of the system, were 73μm and 840μm, respectively. The processors were IFA 655 correlator type analyzers. A frequency shift of 2 MHz, 5 MHz or 10 MHz was applied to discriminate direction. The processor settings were set to at least 5 standard deviations about each side of the mean value to eliminate filter bias.

Flow seeding for LDV consisted of an atomized water-glycerin mixture or Rosco smoke. Seeding was introduced in the plenum to avoid aerodynamic interference. The particle number mean diameter was approximately 4μ m and 1μ m with the water-glycerin and Rosco smoke, respectively. Assuming 100% turbulence intensity, the particle response to velocity fluctuations was estimated through the Stokes number,

$$S = \frac{\tau_P}{\tau_f}$$

where τ_P and τ_f are the particle and fluid relaxation times given by

$$\tau_P = \frac{\rho d^2}{18\mu f}$$

$$\tau_f = \frac{1}{\Omega}$$

$$f = 1 + 0.15\left(\frac{\hat{U}d}{\nu}\right)^{.687}$$

and ρ is the particle density (1200kg/m^3 for water-glycerin), d is the particle diameter (4μ m for water-glycerin), μ and ν are the dynamic and kinematic viscosity of air, $\hat{U}$ is the maximum velocity fluctuation and Ω is the characteristic frequency of the flow (in this case the blade passage frequency). The Stokes number was estimated for the cases studied. The maximum value for S was found to be 0.02. Since this value is below the critical value of 0.1, it can be safely concluded that the particles will follow the flow reliably.

To obtain the three components of velocity, two passes were necessary. The V component was measured during each pass. This redundancy was used to estimate the measurement uncertainty. To access the desired location between the stator and the fan, the system was mounted horizontally at angles of α and β about the x-axis to yield velocities U$_\alpha$ and U$_\beta$, as shown in Figure 1. The physical components could then be determined by vector addition; i.e.,

$$U = U_\alpha \cos(\alpha) - U_\beta \cos(\beta)$$

$$W = U_\alpha \sin(\alpha) + U_\beta \sin(\beta)$$

The total velocity magnitude is given by $\|U\| = (U^2 + V^2 + W^2)^{1/2}$. The mean swirl angle is then given by $\theta = \tan^{-1}(W/U)$.

Measurement uncertainty. The mean velocity measurements were averaged using a transit-time weighting, to correct

2   Copyright © 2002 by ASME

for velocity bias. Preliminary tests were conducted with 10000, 20000, 30000 and 40000 points. Statistical convergence occurred after 15000 points. The particle data rates ranged from 200Hz to 10kHz and were sufficiently high to guarantee bias correction when using transit-time weighting.

The instrument accuracy and positioning resolution during these measurements contributed an uncertainty of 0.008 ‖U‖. The statistical uncertainty (determined from the maximum turbulence level of 100% and a minimum of 500 independent realizations, i.e., blade passages) is estimated to be less than 0.014‖U‖. The flow rate and fan speed were constant to within 0.5% and 10 rpm, respectively. Using the 1986-ASME Uncertainty Standard, for 95% confidence levels, the total uncertainty is estimated to be 0.028‖U‖ on the velocity components. The redundant values obtained for the V component of velocity were verified to lie within this uncertainty bound. The uncertainty for the mean flow angle was thus assessed on the uncertainty of the velocity measurements. The distribution of uncertainty for all measurements is shown as a histogram in Figure 2. The median uncertainty for all measurements could thus be estimated at $\pm 2.2^\circ$ on the mean swirl angle. The uncertainties computed for each velocity and angle measurement are shown as error bars in the relevant figures.
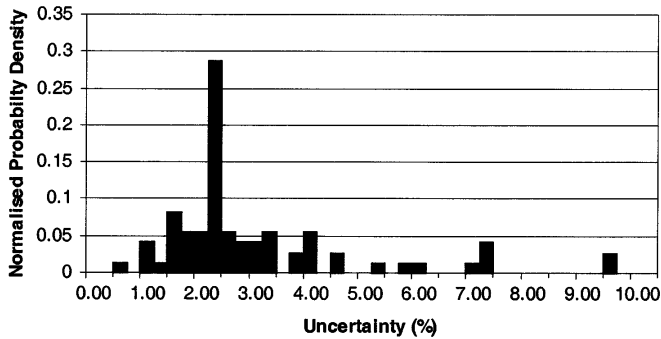

Figure 2. Summary histogram of the LDV experimental uncertainty on swirl angle, θ.

Bias due to uneven particle distribution. Although the transit-time technique does guarantee that the influence of velocity bias will be corrected for sufficiently high data density, the influence of the blade passage may cause uneven particle distribution and thus lead to velocity bias. To verify that this influence is negligible, phase averaging was conducted on several points. Data were accumulated in 100 bins (representing 3.6° of one rotor revolution) and an average value is obtained for each bin. The average value for a fan revolution was then obtained by weighting each bin equally and drawing an ensemble (arithmetic) mean. The two results differed within the ranges indicated by the estimated uncertainty. It can thus be concluded that the results presented here properly account for differences in particle distribution.

Hot-wire anemometry

Hot-wire anemometry was also used to measure the mean and fluctuating velocity field and flow angles. A four-wire probe (AVOP-4-100), shown in Figure 3, manufactured by Auspex Corp., was used to measure the three components of velocity simultaneously. This probe is basically like two X-arrays on the same axis, but rotated 90°. Each of the four wires are inclined 45° from the probe axis, are 1.0 mm long, and 5 μm in diameter. The wires are separated by about 1 mm, so that the effective measurement area is about 1 mm². The probe was connected to four Dantec 90C10 constant temperature anemometers.

Calibration was performed via the Dantec calibration unit. The probes were then carefully moved to the same traversing unit as used by the LDV and connected in exactly the same way. The voltage signals were offset and amplified to minimize A/D errors, and then low-pass filtered at 3000Hz. The voltage signals were sampled at 6000 samples/sec/channel for 40 sec, and stored on disk. The voltages obtained in the wind tunnel were temperature corrected back to the calibration temperature. Using this technique, differences in the mean streamwise velocity when compared to that obtained with a Pitot-static probe in low turbulence flow are typically within 1.0-1.5%.

The probe was calibrated with the approach developed by Wittmer et al. (1998) and is briefly summarized here. Calibration proceeds in two parts with the velocity-voltage calibration (e.g., King's Law), which relates the effective cooling velocities, $U_{eff,i}$ (i=1,4), to the bridge voltages, separated from the directional calibration. The effective velocities are related to approximate velocity components by assuming that they are primarily functions of the velocity normal to the sensors, i.e.,

$$U_{eff,1}^2 = (U_e \sin\theta_1 + V_e \cos\theta_1)^2 + W_e^2$$

$$U_{eff,2}^2 = (U_e \sin\theta_2 + W_e \cos\theta_2)^2 + V_e^2$$

$$U_{eff,3}^2 = (U_e \sin\theta_3 - V_e \cos\theta_3)^2 + W_e^2$$

$$U_{eff,4}^2 = (U_e \sin\theta_4 - W_e \cos\theta_4)^2 + V_e^2$$

These equations are linearized and solved for U_e, V_e, and W_e. Second order effects are accounted for by correction functions, f_j (j=1,3), which are obtained with the directional calibration. The velocity vector is then obtained via

$$V = f_1(V_e/Q_e, W_e/Q_e) * Q_e + V_e$$

$$W = f_2(V_e/Q_e, W_e/Q_e) * Q_e + W_e$$

$$Q = f_3(V_e/Q_e, W_e/Q_e) * Q_e + Q_e$$

3   Copyright © 2002 by ASME

where Q is the magnitude of the velocity vector (i.e., Q = $\|U\|$). Wittmer et al. (1998) assert that the correction functions are robust and therefore do not change much with time, Reynolds number, wire aging, etc. Comparison of those found in the present work, with those in Wittmer et al. (1998) for a nominally similar probe, shows them to be similar, though not precisely the same, giving some evidence to the truth of this statement. Bruun (1995) comments that look-up table approaches, of which this is one, are generally the most accurate to analyzing the voltage signals from the anemometers.
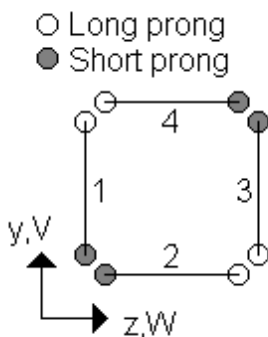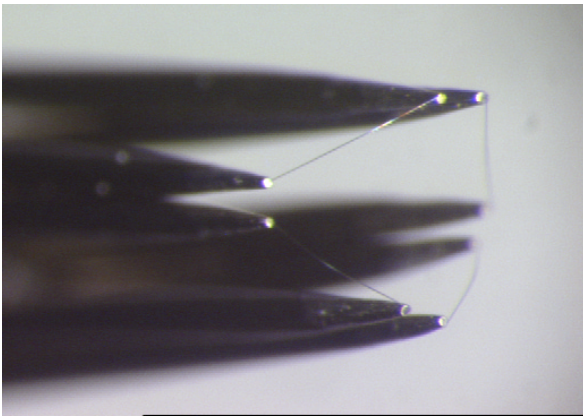

Figure 3. Photograph and schematic sketch of the four-wire probe. Note that x is into the page.

Errors in hot-wire anemometry are due to many factors such as rectification, random calibration errors, wire separation in multi-wire probes, contamination of the sensor by the deposition of impurities from the flow, the signal processing technique, prong or wire vibrations in periodic flows, spatial resolution errors caused by nonuniformity of the flow within the probes sensing volume, temperature fluctuations, aerodynamic disturbances, and human error (Bruun, 1995; Kawall et al, 1983). In general, assessing hot-wire anemometry errors is extremely difficult because the errors themselves are dependent on what precisely is being measured. Errors tend to increase dramatically as the turbulence intensity (the ratio of the streamwise rms. value to the mean velocity) increases over about 30%, primarily due to rectification (see Kawall et al, 1983). Often, simulated numerical data, rather than real data, are used to estimate the magnitudes of error associated with the different factors.

VELOCITY PROFILES AND EXIT ANGLES

LDV results. The measured mean velocity components (U, V, W), the projected velocity magnitude in the x-z plane, $\|U_w\|$, and the total velocity magnitude, $\|U\|$, the mean swirl angle, θ, and are shown in Figures 4 - 6. The error bars indicate the estimated measurement uncertainty.

Results were verified to agree within experimental uncertainty by conducting additional measurement sequences. First, measurements were repeated along the 24°-radius profile (see Fig. 1). The measured velocity component in the horizontal, U_α, and the vertical, U_v, directions, shown in Figure 4, agree within the estimated uncertainty bounds.

The second test consisted of directly comparing the results obtained along the vertical profile. As can be seen from Figures 5 and 6, the two data sets coincide well over most of the range except for three points between radial positions 138mm and 150mm from center. At these locations, there is an interfering stator support member at the vertical position. The bulk of the results clearly indicate that the results are repeatable and verify the validity of the uncertainty analysis. These results also suggest that local flow blockages can have a significant impact on the flow field.

Figure 5 shows that the axial velocity constitutes the principal contribution to the overall velocity magnitude. The flow is generally uniform up to approximately 130mm from the center (9 to 10 m/s) and decreases as the band is approached. The tangential velocity component varies less, from about 3-4m/s from 80mm to 120mm from center to about 5m/s around 130mm from center and decreases towards the band. The flow angle is typically between 15° and 30° over most of the fan area but changes quickly very close to the band, as can be seen in Figure 7.

Comparison of HWA and LDV measurements

The four-wire probe was used to measure the velocity components along the vertical radial line already measured by the LDV. Hot-wire anemometry is generally most accurate when the probe is aligned with the mean flow direction. Since the LDV measurements were made before the HWA measurements, the probe axis was aligned to within about 1 degree of the mean flow direction obtained with the LDV.

The results indicate that there are significant differences when compared with the LDV measurements. The velocity magnitude was about 15% different and the flow angles had differences up to 13°. It is interesting to note, however, that the average value of the measured flow angles differ by only 0.4% between the two techniques. Under normal circumstances, the

4   Copyright © 2002 by ASME

two techniques should match quite closely at every location (as long as the flow is not reversed). In order to determine why these differences exist, the nature of the fluctuating flow field was examined in greater detail. Figures 7 and 8 show the probability density functions (PDF) of the measured flow angles, relative to the probe axis, where

$$\theta_p = \tan^{-1}\left(\frac{w_p}{u_p}\right)$$

$$\phi_p = \tan^{-1}\left(\frac{v_p}{u_p}\right)$$

and the subscript 'p' indicates a probe-based coordinate system. Of particular interest here is θ_p, which is closely related to the instantaneous variability in the swirl angle. Typical turbulent flows, such as wakes, have a distribution with a single peak around some angle which depends on the location in the flow and the flow physics, but is usually near zero since the probe would be normally aligned in the mean flow direction. The present results show that at many radial locations, there are two peaks in the PDFs. In fact, there is a local minima in the probability of occurrence between approximately $-10° < \theta_p < 0°$, i.e., near to where the local maxima normally would be. The most dominant peak generally occurs around $-20°$ to $-30°$. This is very close to the boundary of the allowable approach angle to avoid signal ambiguity problems. In fact, there is signal ambiguity in a range of 6% - 22% of the data at the five radial locations. These extreme points are discarded from the analysis, leading to a bias in the measured flow angles. Assessing the exact magnitude of the bias *a postiori* would be practically impossible without further measurements.

The four-wire probe is only accurate within the flow range for which it was calibrated. Outside of the flow angles calibrated, the voltages yield non-unique solutions for the velocity components and the data point must be discarded both from the calibration and the experiment. From this approach, the allowable range of angles which can be measured is determined. For the present probe, this angle is approximately $30°$, though it depends on the precise direction of the velocity vector. Examining Figure 7, it is clear that there are a considerable number of points near this boundary. This means that the uncertainty in the measured velocity and swirl angle is considerably greater than for the LDV. Assessing the exact uncertainty (or error) is difficult because most existing analyses are based on the velocity fluctuations being Gaussian, or at least approximately so. The bi-modal character of the flow angles downstream of the fan makes an accurate assessment difficult without obtaining further information. More precise measurements could be made by phase-averaging the field and re-orienting the probe for the different phase angles to separately measure the two modes.
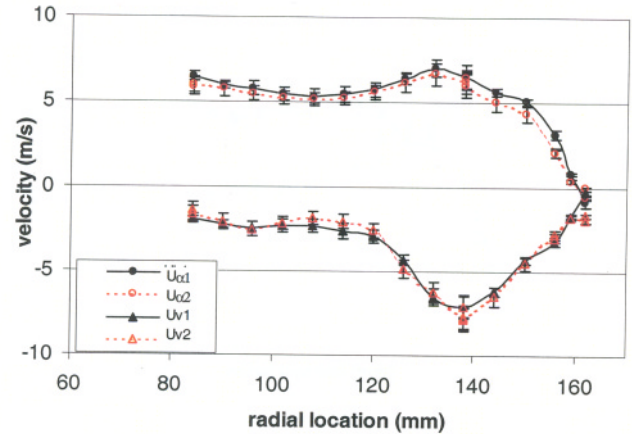

Figure 4. Comparison of measured velocity components in the horizontal, U_α, and vertical, U_v, directions along the $24°$ profile.
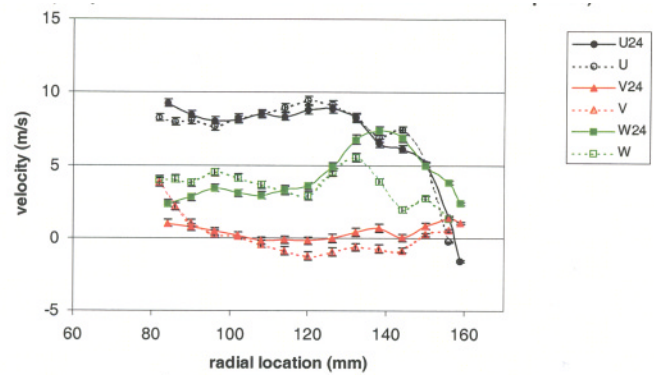

Figure 5. Comparison of measured velocities for radial profiles along the vertical and at a radius at $24°$ from the horizontal plane.
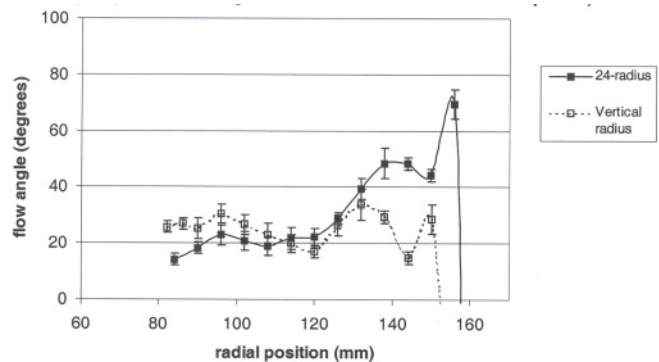

Figure 6. Comparison of measured angles for radial profiles along the vertical and at a radius at $24°$ from the horizontal plane.

CONCLUDING REMARKS

Measurements of the mean velocity vector were conducted to determine the velocity exit angle from an automotive

5   Copyright © 2002 by ASME

radiator-fan-stator assembly. The swirl angle is defined as that subtended by the mean velocity vector relative to the fan axis. The median measured swirl angle uncertainty using the LDV is ±2.2°. The LDV data was verified for consistency and repeatability. The influence of particle density (data rate) on the results was shown to be negligible.
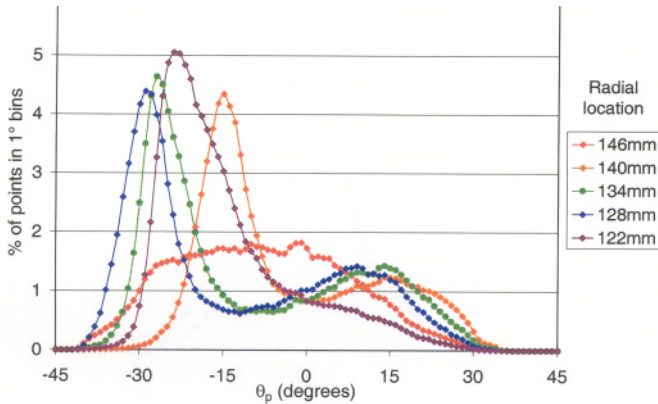

Figure 7. Probability density function of exit flow angles in the x-z plane of the probe as obtained with the four-wire probe.
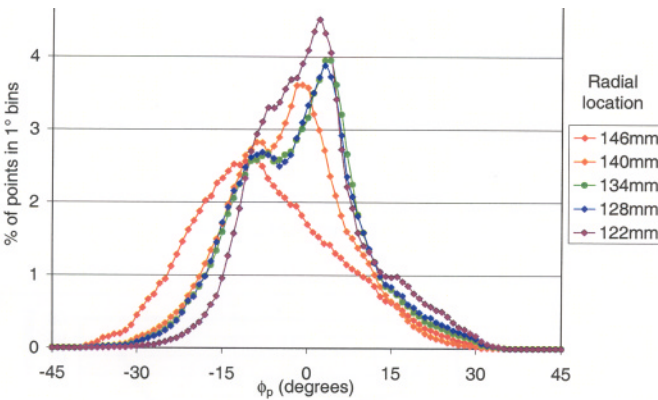

Figure 8. Probability density function of the exit flow angles in the x-y plane of the probe as obtained with the four-wire probe.

The flow angles are defined based on the mean value of the flow velocity. It is not clear that from the design point-of-view that this strategy is optimal. The flow undergoes large variations based on the blade passage. The most probable flow angles are unlikely to be the average flow angles.

It was also found that the results obtained from the present HWA has significant bias errors when used to measure this velocity field. This is because the distribution of swirl angles is bi-modal with the mean flow angle being near a local minimum in the probability density function of the swirl angle. More accurate HWA results could be obtained by adjusting the probe axis by phase.

ACKNOWLEDGEMENTS

REFERENCES

Bruun, HH. 1995 *Hot-Wire Anemometry: Principles and Signal Analysis*, Oxford University Press, Oxford.

Kawall JG, Shokr M & Keffer JF. 1983 A digital technique for the simultaneous measurement of streamwise and lateral velocities in turbulent flows, *J. Fluid Mech*. **133**, 83-112.

Wittmer KS, Devenport WJ & Zsoldos JS. 1998 A four-sensor hot-wire probe system for three-component velocity measurement. *Exp. Fluids* **24**, 416-423.

Copyright © 2002 by ASME